ASSOCIATED VIDEO OPEN

Impaired synaptic transmission and long-term potentiation in severe combined immunodeficient (SCID) mice

Leonardo Lupacchini[a,*], Cristiana Mollinari[b,c,*], Virginia Tancredi[d,e], Enrico Garaci[f] and Daniela Merlo[c]

DNA-dependent protein kinase catalytic subunit (DNA-PKcs) is one of the key enzymes involved in DNA double-strand break (DSB) repair. However, recent studies using DNA-PKcs knockout mice revealed that DNA-PKcs plays an important role in neuronal plasticity. The aim of this study was to examine the role of DNA-PKcs on synaptic plasticity in severe combined immunodeficiency disease (SCID) mice that carry a mutation resulting in a DNA-PKcs protein devoid of kinase activity but still expressed in cells, although with a small COOH-terminal truncation. To this aim, we carried out electrophysiological and molecular analysis on hippocampal slices from wild-type (WT) and SCID mice. Electrophysiological analysis showed an impairment in the basal synaptic transmission in SCID mice compared with WT, whereas paired-pulse facilitation, caused by presynaptic mechanisms, was not different in the two groups of animals. By contrast, tetanic stimulation induced long-term potentiation (LTP) with values that were approximately 43% lower in slices from SCID mice compared with WT. The same slices used for electrophysiology were analyzed to study the phosphorylation state of cAMP response element-binding protein (CREB) and extracellular signal-regulated kinases and to evaluate mRNA expression levels of CREB-target genes at different times after LTP induction. In conclusion, molecular analysis did not show significant differences between SCID and WT brain slices, thus confirming the evidence that DNA-PKcs kinase activity directly regulates neuronal functions and plays a novel role beyond DSB repair. Moreover, these results indicate that studies using SCID mice involving analysis of synaptic function need to be interpreted with caution. ***NeuroReport*** **36: 290–296**

NeuroReport 2025, **36**:290–296

Keywords: cognitive function, DNA-dependent protein kinase catalytic subunit, double-strand breaks, long-term potentiation, severe combined immunodeficiency disease mice, synaptic plasticity

[a]IRCCS, San Raffaele Roma, Via di Val Cannuta, [b]Institute of Translational Pharmacology (IFT), National Research Council, [c]Department of Neuroscience, Istituto Superiore di Sanità, [d]Department of Systems Medicine, 'Tor Vergata' University of Rome, [e]Centre of Space Bio-Medicine, 'Tor Vergata' University of Rome, Rome and [f]San Raffaele Sulmona, Sulmona, Aquila, Italy

Correspondence to Daniela Merlo, PhD, Department of Neuroscience, Istituto Superiore di Sanità, Viale Regina Elena 299, 00161, Rome, Italy
Tel: +39 0649902048; e-mail: daniela.merlo@iss.it

*Leonardo Lupacchini and Cristiana Mollinari contributed equally to the writing of this article.

Received 11 December 2024 **Accepted** 10 February 2025.

Introduction

Severe combined immunodeficiency disease (SCID) mice were first described in 1983 by Bosma *et al*. [1] as a spontaneous homozygous mutation occurring in the BALB/c C.B-17 strain, resulting in an insufficiency of functional B and T cells. SCID mice are diffusely used in biology studies of the immune system and in cancer. Indeed, the absence of a functional immune system makes them a suitable recipient of xenogenic transplants to avoid graft rejection. The syndrome of immunodeficiency in this spontaneous animal model arises from a failure in lymphocyte maturation due to defective V(D)J recombination. Indeed, SCID mice have a homozygous nonsense mutation in the *prkdc* gene, encoding the DNA-dependent protein kinase catalytic subunit (DNA-PKcs), a crucial component of both the DNA double-strand break (DSB) repair machinery and the V(D)J recombination apparatus [2]. The homozygous nonsense mutation at amino acid position 4046 results in the expression of a truncated and enzymatically inactive protein lacking the extreme COOH-terminal region [3]. As a consequence, tissues and cell lines derived from SCID mice exhibit a generalized hypersensitivity to gamma irradiation and a defect in the repair of DSBs [4–6]. Interestingly, reduced levels of DNA-PKcs protein and loss of its activity in the embryonic and postnatal SCID mouse brain induce elevated DSBs and apoptosis in neurons [7]. Indeed, hippocampal neurons from SCID mice exhibit increased vulnerability to DNA damage, oxidative stress, and excitotoxicity, conditions that may occur in neurodegenerative disorders [8].

DNA-PKcs is a member of the phosphatidylinositol 3-kinase (PI3K)-related kinase family, a type of DNA-activated serine/threonine protein kinase, with a molecular weight of approximately 460 kDa [9] that forms the

Related digital media are available in the full-text version of the article at www.neuroreport.com.

active holoenzyme by binding to the Ku80/Ku70 heterodimers [10]. Recent studies revealed that DNA-PKcs participates in signal transduction cascades related to different pathways including apoptotic cell death, telomere homeostasis, mitochondrial health, metabolism, autophagy, transcription, protein stability, and RNA binding, thus identifying new physiological functions, beyond genome stability.

We have recently published that DNA-PKcs has an important modulatory role in synaptic plasticity via postsynaptic protein-95 (PSD-95) phosphorylation. In particular, DNA-PKcs localizes at synapses, responds to synaptic stimuli, interacts with different postsynaptic proteins, and phosphorylates PSD-95 at newly identified and evolutionary conserved amino acids thus controlling PSD-95 protein stability. We also showed that DNA-PKcs knockout mice, lacking both protein and enzymatic activity, present a deficit in long-term potentiation (LTP) along with changes in neuronal morphology, and reduced levels of different postsynaptic proteins [11].

To differentiate the contribution of DNA-PKcs as kinase from its role as protein scaffold at the synapses, here we used SCID mice lacking DNA-PKcs kinase activity but still maintaining intact most of the entire DNA-PKcs protein.

We investigated synaptic functions, plasticity-related protein activation, and immediate early genes (IEGs) expression involved in synaptic plasticity. We found that SCID mice show impaired LTP, whereas we did not find any difference neither in the activation of downstream proteins nor in the IEGs expression, suggesting that SCID mice show similar features to those of DNA-PKcs knockout mice.

Moreover, our findings show for the first time that, due to DNA-PKcs novel synaptic role, when SCID mice are used to conduct brain function studies, the results may be misinterpreted.

Material and methods

Animals

Animal procedures were carried out according to the European Community Guidelines for Animal Care, DL 26/2014, application of the European Communities Council Directive, 2010/63/EU, Federation of European Laboratory Animal Science Associations and Animal Research: Reporting of In Vivo Experiments guidelines, and approved by the Italian Ministry of Health and by the local Institutional Animal Care and Use Committee.

The Fox Chase SCID mice (CB17/Icr-*Prkdc*^{scid}/IcrIcoCrl) (Charles River, Milan, Italy) that possess a genetic autosomal recessive mutation designed *Prkdc*^{SCID} were kept in a pathogen-free environment, in individually ventilated cages under standard conditions. Animal studies were approved and permission was issued by 'Ministero della Salute' (Approval number DM 90/2016-PR to D.M.).

Electrophysiology

Transverse hippocampal slices (500 μm) were incubated in an interface chamber at 32 °C–33 °C, superfused with oxygenate artificial cerebrospinal fluid containing 124 mM NaCl, 2 mM KCl, 1.8 mM $MgSO_4$, 2 mM $CaCl_2$, 26 mM $NaHCO_3$, 1 mM NaH_2PO_4, and 10 mM glucose, and allowed to equilibrate for at least 60 min. Field excitatory postsynaptic potentials (fEPSP) in the hippocampus were recorded in the *stratum radiatum* of the CA1 with a glass microelectrode upon stimulation of Schaffer collaterals. Paired-pulse facilitation (PPF) was assessed by applying a pair of Schaffer collateral stimuli at intervals of 10–125 ms, and the ratio of slopes of the second to the first response was calculated, so that numbers greater than 1.0 represented facilitation.

Responses were characterized by the application of paired-pulse stimulation (PPS, two consecutive pulses 50-ms apart), and only fEPSP showing PPF (R2/R1 ratio ≥1) were used for recording. Paired-pulse ratio (PPR) was used as an indicator inversely proportional to presynaptic neurotransmitter release [12]. After PPS, during conventional recording, each pulse was delivered every 20 s (square pulses of 100 μs duration at a frequency of 0.05 Hz), and three consecutive responses were averaged.

LTP was induced by stimulating Schaffer collaterals with a high-frequency stimulation (HFS) protocol consisting of one single train (100 Hz, 1 s) [13].

Western blot analysis

After electrophysiological recordings, hippocampal individual slices, using a brush, were immediately placed on a petri dish with ice underneath the dissecting microscope. Then, using a scalpel, the CA1 region was dissected out and rapidly frozen in liquid nitrogen. Subsequently, tissues were homogenized in ice-cold buffer containing 50 mM Tris-HCl, 150 mM NaCl, 10 mM EDTA, 1 mM phenylmethylsulfonyl fluoride, 1% Triton X-100, 0.1% SDS, 0.5% deoxycholic acid sodium salt, and protease and phosphatase inhibitors (Sigma, Milan, Italy). All slices used for biochemical analysis were monitored electrophysiologically. Proteins (30–80 μg) were subjected to 5 or 10% polyacrylamide gels SDS-PAGE depending on the molecular weight of the proteins to be analyzed [5% polyacrylamide for DNA-PKcs, and Hsp90 or 10% for extracellular signal-regulated kinases (ERK1/2), cAMP response element-binding protein (CREB)]. After electrophoresis, proteins were transferred onto nitrocellulose membranes (Amersham Biosciences, Cologno Monzese, Italy). After blocking, membranes were incubated overnight at 4 °C with primary antibodies and then with the appropriate horseradish peroxidase-conjugated secondary antibody for 1 h at room temperature. The following primary antibodies were used: DNA-PKcs antibody

(Ab-4, Neo Markers, Milan, Italy), a mixture of 3 monoclonal antibodies: clone 18-2, clone 25-4, clone 42psc. Clone 18-2 was raised against DNA-PKcs protein region (1–2713 aa); clone 25-4 against DNA-PKcs protein region (3198–4127 aa), and finally clone 42psc recognizes the C-terminal 150 kDa of DNA-PKcs; phospho-ERK1/2 (Thr202/Tyr204); total ERK1/2; phospho-CREB (Ser133); total CREB (Cell Signaling Technology, Cambridge, UK), and Hsp90-alpha (ABCAM, Milan, Italy). Proteins were visualized using an enhanced chemiluminescence detection system (EuroClone, Milan, Italy) ECL. Images were acquired using an Amersham ImmageQuant 800 (GE Healthcare, Milan, Italy), and densitometric analysis was performed using ImageQuant software (GE Healthcare) and Fiji Image software (NIH, Bethesda, Maryland, USA).

Real-time PCR

Total RNA was prepared from CA1 dissected hippocampal slices using the Paris kit (Invitrogen). Total RNA (1 µg) was reverse transcribed using the first-strand synthesis system for real-time PCR (Superscript, Invitrogen, Milan, Italy). Relative real-time PCR was performed in a Real-Time Thermocycler (MX 3000, Stratagene, Milano, Italy) using the Brilliant SYBR Green QPCR Master Mix as described in [14]. Quantitative data were normalized to the expression of housekeeping gene 18S rRNA. Specific primers for mouse c-Fos, Egr-1, Exon-III containing BDNF transcript, BDNF, and 18S rRNA were designed to amplify short DNA fragments.

(18S forward 5'-GTAACCCGTTGAACCCCATT-3'; 18S reverse 5'-CCATCCAATCGGTAGTAGCG-3'; c-Fos forward 5'-ATCGGCAGAAGGGGCAAAGTAG-3'; c-Fos reverse 5'-GCAACGCAGACTTCTCATCTTCAAG-3'; Egr-1 forward 5'-CCTATGAGCACCTGACCACA-3'; Egr-1 reverse 5'-AGCGGCCAGTATAGGTGATG-3'; Exon-III BDNF forward 5'-TATCATCCCTCCCCGAGAGT-3'; Exon-III BDNF reverse 5'- CTGGGCTCAAGGAAGCAT-3'; BDNF forward 5'-TGCGAGTATTACCTCCGCCA-3'; BDNF reverse 5'-TGACGTGCTCAAAAGTGTCA-3). The relative quantitation was calculated with the analysis software that accompanied the thermal cycler.

Statistical analysis

Throughout the text, measurements are expressed as mean ± SEM. Statistical differences between two groups were evaluated with an unpaired two-tailed Student's *t* test. Two-way ANOVA was used for the multiple comparisons followed by post-hoc tests. The exact *p* values are provided unless it is at least $P < 0.05$, accepted as the level of significance for all of the tests.

Results

Severe combined immunodeficient mice show impairment in synaptic transmission and long-term potentiation

We first confirmed the expression of DNA-PKcs in total extracts from the cortex of SCID mice, compared with wild-type (WT) mice. Western blot in Fig. 1a shows that DNA-PKcs expression is reduced in SCID brain, probably due to the fact that the truncated DNA-PKcs, lacking approximately 8 kDa of the COOH-terminal region, is a less stable protein [3,15].

We then performed electrophysiological analysis in SCID mice, at 8 weeks of age, by recording extracellular field potentials in the CA1 area of hippocampal slices, after stimulation of the Schaffer collaterals (Fig. 1b–e). We first evaluated basal synaptic transmission and found a statistical significant difference in input/output (I/O) curves between SCID and WT mice, with a lower averaged fEPSP slope in SCID ($n = 5$) with respect to WT mice ($n = 6$) at the highest stimulus intensity (Fig. 1b), indicating an impairment in basal synaptic transmission in SCID mice ($^{*}P < 0.05$).

We further measured PPF in SCID mice, and PPR was used as an indicator inversely proportional to presynaptic neurotransmitter release [12] (Fig. 1c). We found no significant differences in the PPF between SCID ($n = 6$) and WT ($n = 5$), indicating that presynaptic mechanisms are not affected in SCID (WT: 1.62 ± 0.087; SCID: 1.51 ± 0.080; $P = 0.3781$) (Fig. 1c, d).

We then evaluated the induction of LTP, by stimulating Schaffer collaterals with a HFS protocol consisting of 1 train (100 Hz, 1 s). In WT mice ($n = 12$), HFS-induced LTP measured 50 min after HFS, as a potentiation of fEPSP slope (143.74 ± 11.83% of basal value). On the contrary, in SCID mice ($n = 12$), HFS did not potentiate fEPSP (100.18 ± 9.67% of basal value) (WT vs. SCID $^{**}P < 0.005$) (Fig. 1e).

Severe combined immunodeficient mice show normal synaptic plasticity-related signaling pathways

After electrophysiological recordings, a single slice from a single mouse (WT or SCID) was rapidly dissected to isolate the CA1 region. Frozen lysates from CA1 regions were analyzed by Western blot to study phosphorylation changes of synaptic plasticity-related proteins such as CREB and ERK1/2 at different time points after delivering of HFS in WT ($n = 3$) and SCID mice ($n = 3$) [11,16]. Densitometric quantification of the immunoreactive bands indicates no significant differences in phosphorylation levels of CREB and ERK1/2 between WT and SCID CA1 slices at the different time points analyzed (T2' CREB: WT: 203 ± 20.25%, SCID: 174.33 ± 6.33%; $P = 0.8129$; $n = 4$ mice; T5' CREB: WT: 591.33 ± 8.81%, SCID: 573.33 ± 29.53%; $P = 0.9792$; $n = 4$ mice; T15' CREB: WT: 215.33 ± 7.68%, SCID: 226.66 ± 6.74%; $P = 0.9987$; $n = 4$ mice; T5' ERK1/2: WT: 277 ± 15.53%, SCID: 264.66 ± 20.79%; $P = 0.991$; $n = 3$ mice; T15': WT: 348 ± 51.50%, SCID: 245.33 ± 18.94%; $P = 0.104$; $n = 3$ mice) (Fig. 2).

We then analyzed, by Real-Time PCR, the mRNA expression levels of some IEGs known to be actively

Fig. 1

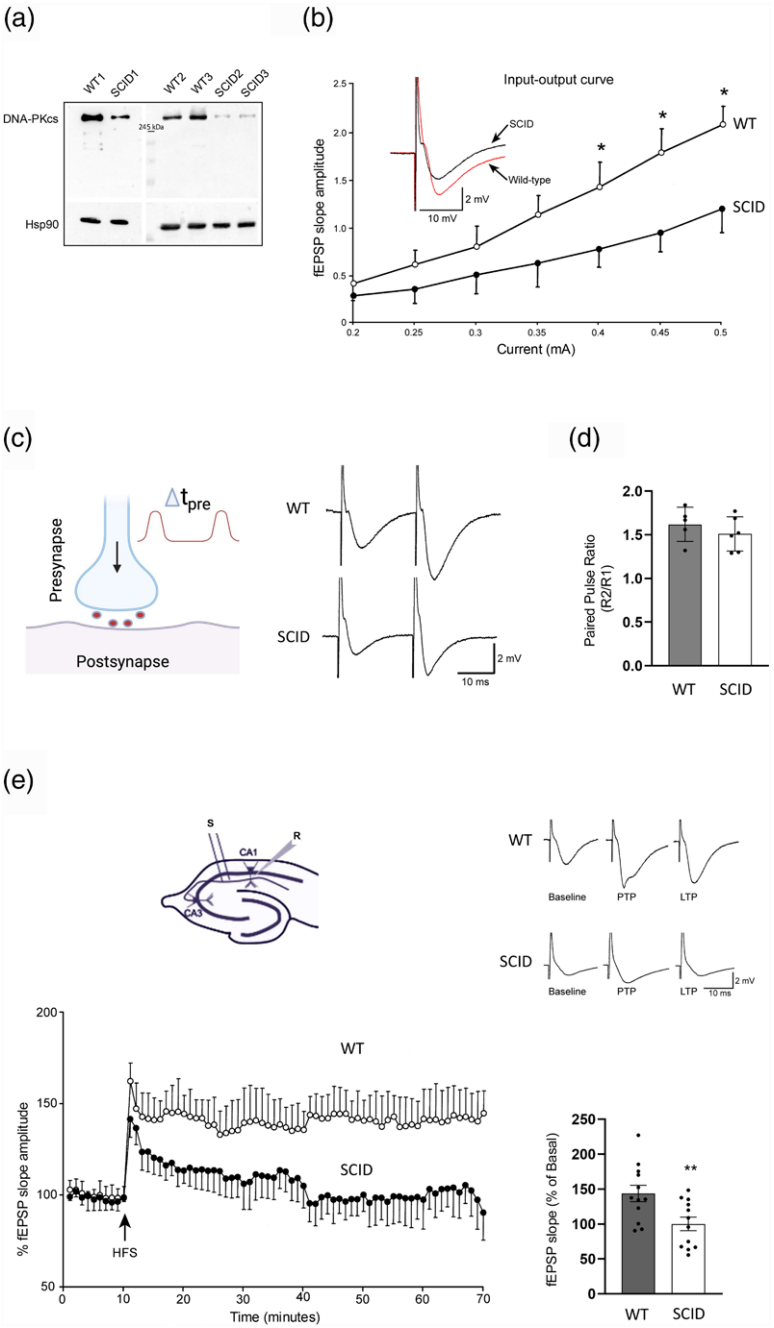

(a) Western blot analysis showing a strong reduction of DNA-PKcs protein expression levels in extracts of brain cortex from WT and SCID mice. Hsp90 was used as a loading control. (b) Representative fEPSPs evoked in response to successive increments of current intensity in WT and SCID hippocampal slices. Input–output curves of fEPSP slope against stimulus intensity show a deficient synaptic transmission in SCID mice (black circles) as compared with WT. (white circles). All points between 0.4 and 0.5 mA are significantly different between the two experimental groups ($P < 0.05$). (c) Left panel: A schematic diagram of the short-term synaptic plasticity protocol to induce PPF. Right panel: Examples of PPF traces triggered by a pair of presynaptic spikes with a Δ tpre = 50 ms from WT and a SCID stimulated hippocampal slices. Scale bars represent 2 mV by 10 ms for both traces. (d) The histogram shows the ratio R2/R1, plotted as a function of interspike interval, Δ tpre, between two successive presynaptic spikes. No significant difference was detected between the two groups (WT $n = 5$, SCID $n = 6$) (WT: 1.62 ± 0.087; SCID: 1.51 ± 0.080; $P = 0.3781$). Histogram data are presented as mean ± SEM of the facilitation of the second fEPSP response relative to the first response. (e) Upper left: Representative graph indicating sites of stimulating and recording electrodes in a mouse hippocampus sagittal section. Upper right: Two examples of recordings of WT and SCID mice depicted at the basal synaptic response, 1 and 40 min after HFS protocol. Scale bars represent 2 mV by 10 ms for both traces. Lower left: High-frequency stimulation (1 train at 100 Hz, 1 s) induces LTP with a higher magnitude in WT hippocampal slices compared with SCID mice. Lower right: Histogram shows a significant difference in the magnitude of LTP in WT and SCID hippocampus slices. The normalized fEPSP slope for WT mice 50 min after the tetanus is 143.74 ± 11.83% of the mean slope before stimulation and that for SCID mice is 100.18 ± 9.67% of the basal value (WT vs. SCID $^{**}P < 0.005$) (WT $n = 12$; SCID $n = 12$). Data represent mean (±SEM). Statistics by Student's t test (unpaired, two-tailed). DNA-PKcs, DNA-dependent protein kinase catalytic subunit; fEPSP, field excitatory postsynaptic potentials; HFS, high-frequency stimulation; LTP, Long-Term Potentiation; PPF, Pair Pulse Facilitation; SCID, severe combined immunodeficiency disease; WT, wild type.

Fig. 2

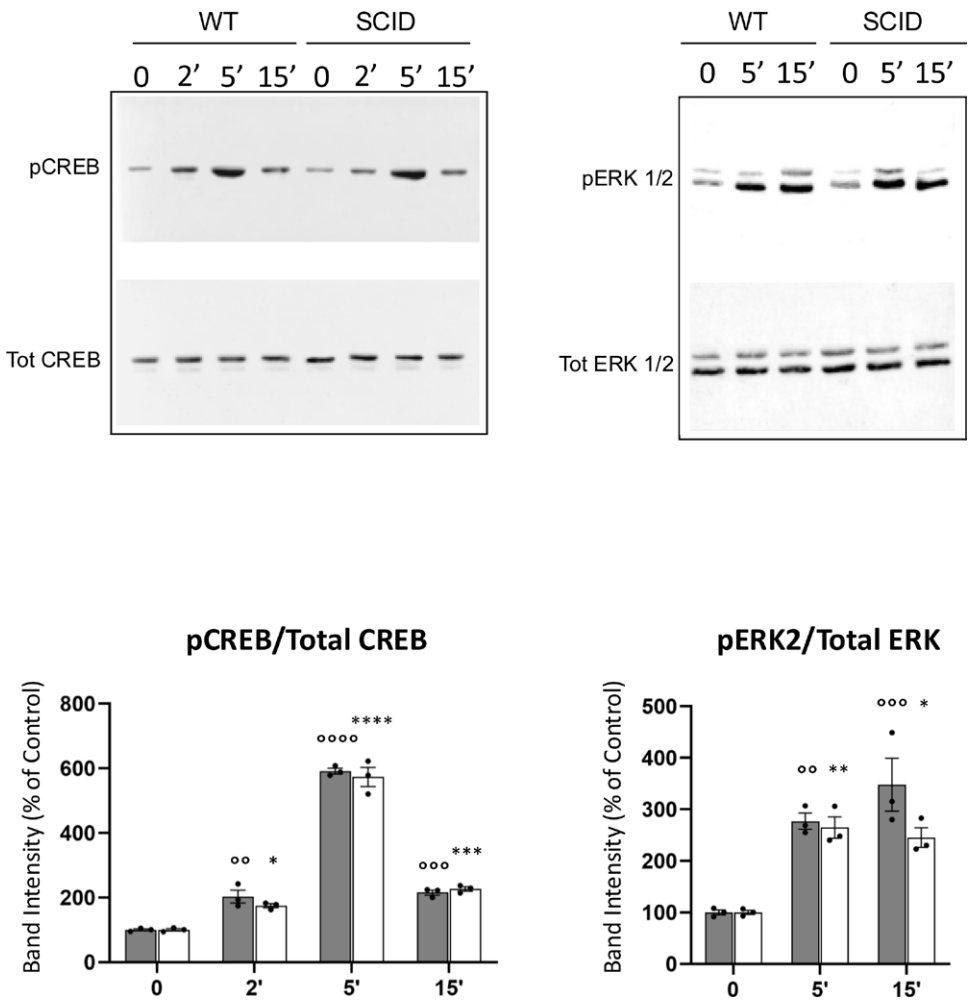

Representative Western blots of phosphorylated and total forms of CREB and ERK1/2 at different times after delivery of HFS. Values in the plots represent the percent changes in protein phosphorylation, normalized to the total protein, with respect to control (T0) for each time point. CREB: °°$P < 0.005$ WT T2' control values (T0), °°°°$P < 0.0001$ WT T5' control values (T0), °°°$P < 0.001$ WT T15' control values (T0), SCID T2' *$P < 0.05$ vs. control values (T0), SCID T5' ****$P < 0.0001$ vs. control values (T0), SCID T15' ***$P < 0.001$ vs. control values (T0). ERK1/2: °°$P < 0.005$ WT T5' control values (T0), °°°$P < 0.001$ WT T15' control values (T0), SCID **$P < 0.005$ SCID T5' control values (T0), SCID *$P < 0.05$ T15' vs. control values (T0). Data represent mean (±SEM) and were analyzed by two-way ANOVA followed by Tukey's post-hoc analysis. CREB, cAMP response element-binding protein; ERK1/2, extracellular signal-regulated kinases; HFS, high-frequency stimulation; SCID, severe combined immunodeficiency disease; WT, wild type.

transcribed following synaptic stimulation in CA1 dissected regions at different times after LTP [16]. The following transcripts were evaluated: c-Fos, Egr-1, Exon-III BDNF, and total BDNF. No significative differences were found in the expression levels of mRNAs for any genes analyzed between WT and SCID hippocampal stimulated slices ($n = 4$ for both experimental groups) (Fig. 3).

Discussion

The main result of the present study is that SCID mice show an impairment in LTP similar to the later-developed DNA-PKcs knockout mice in which a 260 aa truncation results in loss of the entire kinase domain [15]. On the contrary, SCID mutation truncates only the extreme COOH-terminus of the protein by approximately 8 kDa, unique to the PI3K-related subfamily, thus leaving most of the entire DNA-PKcs protein intact but abolishing the ability of DNA-PKcs to function as a kinase [3]. Although this mutation results in a decrease in DNA-PKcs protein levels, it can be detected in SCID cell lines of different origin [3,7]. Accordingly, Western blot analysis in the present study shows the presence of a protein with the expected molecular weight of 460 kDa in brain tissue. Therefore, the SCID mouse model can be extremely valuable to studying DNA-PKcs functions in the brain particularly because it can allow us to differentiate the contribution of DNA-PKcs' scaffold from its

Fig. 3

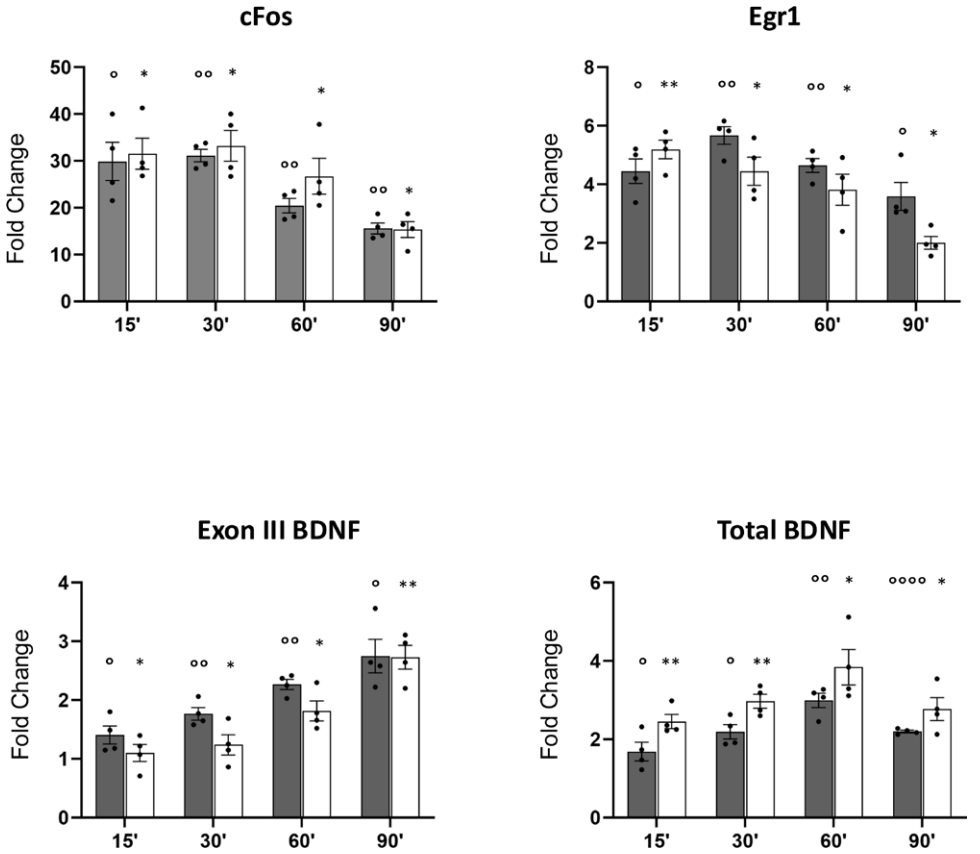

Real-time PCR analysis of: c-Fos, Egr-1, Exon-III BDNF, and total BDNF mRNAs. Histogram data represent the fold change of IEG mRNAs at different time intervals after HFS in CA1-stimulated hippocampal slices of WT and SCID mice ($n = 4$ for each group). Values represent mRNA fold changes, normalized to 18S rRNA, with respect to control (T0) for each time point. Data represent mean (±SEM) and were analyzed by two-way ANOVA followed by Tukey's post-hoc analysis. For the IEGs: c-Fos: °$P < 0.05$ WT T0 vs. T15', °°$P < 0.005$ WT T0 vs. T30', T60', and T90'; *$P < 0.05$ SCID T0 vs. T15', T30', T60', and T90'. Egr-1: °$P < 0.05$ WT T0 vs. T15' and T90'; °°$P < 0.005$ WT T0 vs. T30' and T60'; *$P < 0.05$ SCID T0 vs. T30', T60', and T90', **$P < 0.005$ SCID T0 vs. T15'. Exon-III BDNF: °$P < 0.05$ WT T0 vs. T15' and T90', °°$P < 0.005$ WT T0 vs. T30' and T60'; *$P < 0.05$ SCID T0 vs. T15', T30', and T60', **$P < 0.005$ SCID T0 vs. T90'. Total BDNF: °$P < 0.05$ WT T0 vs. T15' and T30', °°$P < 0.005$ WT T0 vs. T60', °°°°$P < 0.0001$ WT T0 vs. T90'; *$P < 0.05$ SCID T0 vs. T60' and T90', **$P < 0.005$ SCID T0 vs. T15' and T30'. BDNF, brain-derived neurotrophic factor; IEG, immediately early gene; SCID, severe combined immunodeficiency disease; WT, wild type.

enzymatic activity. Indeed, in light of its large size, one interesting possibility is that DNA-PKcs plays a structural role. As a scaffolding protein, it can interact with several other factors and hold them in appropriate orientations with respect to one another to facilitate interactions and condensation in specific cellular sites including the synapses. This hypothesis is in line with recent studies showing that kinases lacking one or more of the amino acids typically required to correctly align ATP and metal ions show the biological relevance of pseudokinases, which are now thought to perform a range of physiological roles and are also connected to several human diseases including neurodegeneration [17]. However, the similarity of our results obtained with DNA-PKcs knockout mice and SCID mice confirms a direct role of DNA-PKcs kinase activity and not of its scaffold in LTP, but leaves open the possibility of new functions not directly linked to its enzymatic activity that can be revealed by using SCID model.

In this study, we also analyzed some plasticity-related canonical pathways. In agreement with our previous results, the phosphorylation state of ERK1/2 increased 5 min following LTP induction, remaining sustained for at least 15 min [11,16], and was NS different between SCID and WT mice. Furthermore, we studied the phosphorylation level of CREB at serine 133, which represents another major posttranslational modification essential to learning and memory. We found that CREB phosphorylation was increased 2 min after LTP induction, with a strong increment at 5 min that lasted 15 min, as previously reported [16]. We also investigated the transcription of CREB-target genes in potentiated slices. We found that CREB phosphorylation is associated with a consistent increase in the expression of c-fos, Egr-1, and exon-III containing BDNF transcript that persisted for at least 90 min after tetanic stimuli. All together these molecular findings show that the timing of phosphorylation and expression of the major molecules involved in LTP are

unaltered in the absence of DNA-PKcs kinase activity, thus confirming that DNA-PKcs acts independently during LTP and regulates synaptic plasticity via PSD-95 phosphorylation and stability [11].

SCID mice are commonly used for immunological studies due to the lack of functional immune cells; however, they possess other cellular features directly linked to the genetic defect of DNA-PKcs. Indeed, SCID cells and neurons are hypersensitive to ionizing radiation, and cell-cycle abnormalities have also been demonstrated in the regenerating liver of SCID mice [18]. In addition, SCID mice show an increased number of microglia in hippocampal and cerebellar brain regions [19], increased apoptosis in cortical neurons [7], and increased vulnerability to DNA damage, oxidative stress, and excitotoxicity of hippocampal neurons [8].

Therefore, although SCID mice may prove to be a powerful tool for studying new roles of DNA-PKcs in the central nervous system, it is important to emphasize that studies using SCID mice focusing on brain functions must take into account the role of DNA-PKcs in neuronal cells and synaptic plasticity.

Conclusions

DNA-PKcs has long been studied and appreciated for its role in DNA DSB repair mechanism, but recent evidence highlights new roles of this kinase beyond its initial DNA reparative function. Thus, it is possible that our understanding of DNA-PKcs is far from being complete. Here, we provide evidence that SCID mice may help to elucidate the function of DNA-PKcs in the nervous system.

Further studies will help to identify molecules and signaling pathways, regulating DNA-PKcs activity, which may have therapeutic potential for reducing synaptic loss and cognitive impairment in different neurological diseases.

Acknowledgements

This study has been supported by the Italian Ministry of Health (Ricerca Corrente 10/2405 to L.L.). Figure 1c was created with BioRender.com (Agreement number FU27MFJIC0).

Conflicts of interest

There are no conflicts of interest.

References

1 Bosma GC, Custer RP, Bosma MJ. A severe combined immunodeficiency mutation in the mouse. *Nature* 1983; **301**:527–530.
2 Blunt T, Finnie NJ, Taccioli GE, Smith GC, Demengeot J, Gottlieb TM, *et al*. Defective DNA-dependent protein kinase activity is linked to V(D)J recombination and DNA repair defects associated with the murine scid mutation. *Cell* 1995; **80**:813–823.
3 Beamish HJ, Jessberger R, Riballo E, Priestley A, Blunt T, Kysela B, Jeggo PA. The C-terminal conserved domain of DNA-PKcs, missing in the SCID mouse, is required for kinase activity. *Nucleic Acids Res* 2000; **28**:1506–1513.
4 Fulop GM, Phillips RA. The scid mutation in mice causes a general defect in DNA repair. *Nature* 1990; **347**:479–482.
5 Biedermann KA, Sun JR, Giaccia AJ, Tosto LM, Brown JM. scid mutation in mice confers hypersensitivity to ionizing radiation and a deficiency in DNA double-strand break repair. *Proc Natl Acad Sci U S A* 1991; **88**:1394–1397.
6 Hendrickson EA, Liu VF, Weaver DT. Strand breaks without DNA rearrangement in V (D)J recombination. *Mol Cell Biol* 1991; **11**:3155–3162.
7 Vemuri MC, Schiller E, Naegele JR. Elevated DNA double strand breaks and apoptosis in the CNS of scid mutant mice. *Cell Death Differ* 2001; **8**:245–255.
8 Culmsee C, Bondada S, Mattson MP. Hippocampal neurons of mice deficient in DNA-dependent protein kinase exhibit increased vulnerability to DNA damage, oxidative stress and excitotoxicity. *Brain Res Mol Brain Res* 2001; **87**:257–262.
9 Hartley KO, Gell D, Smith GC, Zhang H, Divecha N, Connelly MA, *et al*. DNA-dependent protein kinase catalytic subunit: a relative of phosphatidylinositol 3-kinase and the ataxia telangiectasia gene product. *Cell* 1995; **82**:849–856.
10 Gottlieb TM, Jackson SP. The DNA-dependent protein kinase: requirement for DNA ends and association with Ku antigen. *Cell* 1993; **72**:131–142.
11 Mollinari C, Cardinale A, Lupacchini L, Martire A, Chiodi V, Martinelli A, *et al*. The DNA repair protein DNA-PKcs modulates synaptic plasticity via PSD-95 phosphorylation and stability. *EMBO Rep* 2024; **25**:3707–3737.
12 Schultz W. Predictive reward signal of dopamine neurons. *J Neurophysiol* 1998; **80**:1–27.
13 D'Arcangelo G, Grossi D, Racaniello M, Cardinale A, Zaratti A, Rufini S, *et al*. Miglustat reverts the impairment of synaptic plasticity in a mouse model of NPC disease. *Neural Plast* 2016; **2016**:3830424.
14 Mollinari C, Ricci-Vitiani L, Pieri M, Lucantoni C, Rinaldi AM, Racaniello M, *et al*. Downregulation of thymosin beta4 in neural progenitor grafts promotes spinal cord regeneration. *J Cell Sci* 2009; **122**:4195–4207.
15 Taccioli GE, Amatucci AG, Beamish HJ, Gell D, Xiang XH, Torres Arzayus MI, *et al*. Targeted disruption of the catalytic subunit of the DNA-PK gene in mice confers severe combined immunodeficiency and radiosensitivity. *Immunity* 1998; **9**:355–366.
16 Racaniello M, Cardinale A, Mollinari C, D'Antuono M, De Chiara G, Tancredi V, Merlo D. Phosphorylation changes of CaMKII, ERK1/2, PKB/Akt kinases and CREB activation during early long-term potentiation at Schaffer collateral-CA1 mouse hippocampal synapses. *Neurochem Res* 2010; **35**:239–246.
17 Mace PD, Murphy JM. There's more to death than life: noncatalytic functions in kinase and pseudokinase signaling. *J Biol Chem* 2021; **296**:100705.
18 Watanabe F, Shinohara K, Teraoka H, Komatsu K, Tatsumi K, Suzuki F, *et al*. Involvement of DNA-dependent protein kinase in down-regulation of cell cycle progression. *Int J Biochem Cell Biol* 2003; **35**:432–440.
19 Lorke DE, Ip CW, Schumacher U. Increased number of microglia in the brain of severe combined immunodeficient (SCID) mice. *Histochem Cell Biol* 2008; **130**:693–697.